Nuclear Engineering and Design 350 (2019) 147–157

Contents lists available at ScienceDirect

Nuclear Engineering and Design

journal homepage: www.elsevier.com/locate/nucengdes

Enhancement of seismic resilience of piping systems in nuclear power plants using steel coil damper

Sung Gook Cho[a,*], Osamu Furuya[b], Hiroshi Kurabayashi[c]

[a] R&D Center, Innose Tech Co., Ltd, Republic of Korea
[b] Division of Mechanical Engineering, Tokyo Denki University, Japan
[c] Vibro-System, Japan

ARTICLE INFO

Keywords:
Piping system
Design basis earthquake
Elasto-plastic steel coil spring damper
Vibration control
Seismic margin

ABSTRACT

After the accident at Fukushima, it has become more a mandatory to enhance the safety level of nuclear power plants (NPPs). It has been suggested that the piping systems in NPPs should be improved as part of measures to mitigate severe accidents that may occur when the earthquake ground input motion exceeds the level of the design basis earthquake (DBE). In this study, a steel coil damper (SCD) has been proposed to reduce the vibration of the piping system and ensure the safety of the NPP when a seismic event exceeds the DBE. This study developed an analytical model and design method for the SCD. The basic mechanical characteristics of the SCD were verified through experiments on the specimens designed and manufactured according to design equations developed in this study. The proposed analytical model of SCD is compared with the mechanical characteristics obtained from the experiments. Test results agree well with the analytical mechanical characteristic of the SCD. The actual seismic margin of the piping system with SCDs was evaluated by the analyses. The study results prove that the proposed damper is effective at maintaining the function and ensuring the safety of the NPP under extreme conditions.

1. Introduction

There has been acquisition of new and important seismic engineering knowledge from recent major earthquakes. There was almost no damage to equipment and piping, which are classified as seismic importance class, though more than two times the level of input motion beyond the design earthquake was induced on nuclear structures in Japan (Miyano et al., 2009). This fact verified the effectiveness of the seismic margin possessed by all sorts of machines and structures belonging to the nuclear facilities. Also, it revealed a large task: that actual seismic capacity should be evaluated for critical equipment and piping from the viewpoint of maintaining the function of nuclear systems over the entire nuclear industry.

From an engineering point of view, it is very difficult to understand the relationship between actual capacity and seismic margin of nuclear system, which are composed of complex equipment and piping systems, because so far there is lots of uncertainty in mechanical structures and epistemic uncertainty in the civil structures. Evaluation of actual capacity for a system composed of equipment and piping becomes more significant in relation to the implementation of margin evaluation by probabilistic risk assessment against earthquakes as external events. However, professional knowledge for actual capacity of partial damage inside a system is quite unobtainable. In this situation, Japan has begun to verify the function of critical equipment and to assess their actual seismic capacity by using a shaking table that can excite an object at up to 20.0 g (Sakai et al., 2016; Kojima et al., 2017, 2018).

The vibration of the piping system in NPPs is affected by various loads including earthquake motion. Pipes and pipe support structures deform plastically to become permanently deformed when they are vibrated by a huge earthquake (Takahashi and Maekawa, 2012). The actual damping value of the piping system including the support structure increases as the level of input motion increases (Takahashi and Maekawa, 2014). Nakamura (2013) performed shaking table testing to study the seismic safety capacity of piping system with support structures.

According to the limitation of the primary stress, as the level of design ground motion increases, more support devices like snubbers and hangers are installed on the piping system to enhance the seismic capacity. However, there are many uncertainties about the marginal capacity of the supporting systems that are provided against beyond DBE (BDBE). It is important to investigate the failure mode of the piping system under BDBE. If a piping system is subjected to an input motion

* Corresponding author.
E-mail addresses: sgcho@innose.co.kr (S.G. Cho), osamu.furuya@mail.dendai.ac.jp (O. Furuya), h-kura@os.rim.or.jp (H. Kurabayashi).

https://doi.org/10.1016/j.nucengdes.2019.05.006
Received 22 November 2018; Received in revised form 9 April 2019; Accepted 7 May 2019

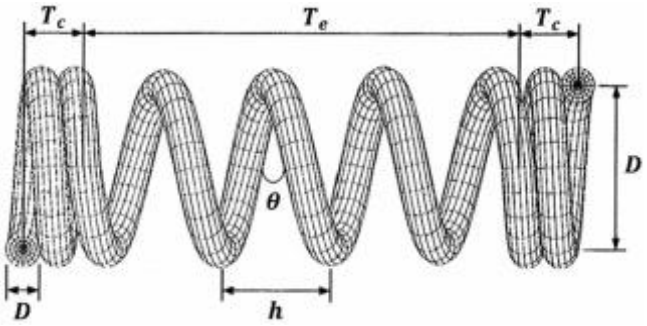

Fig. 1. Dimension of elasto-plastic coil damper.

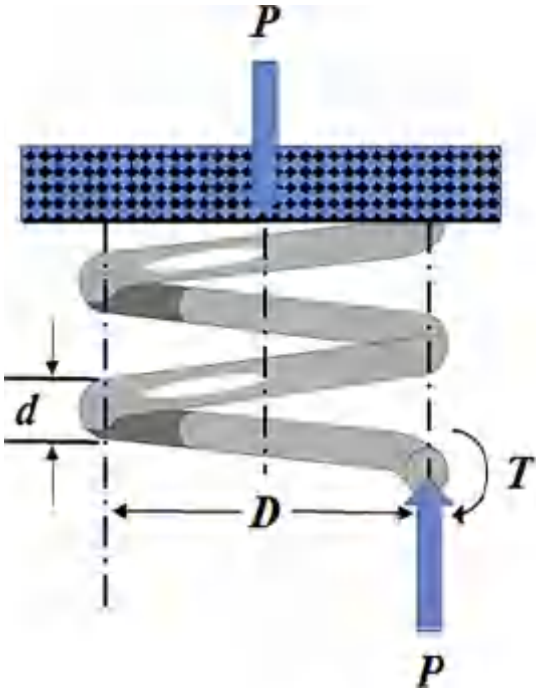

Fig. 2. Forces in compressive spring.

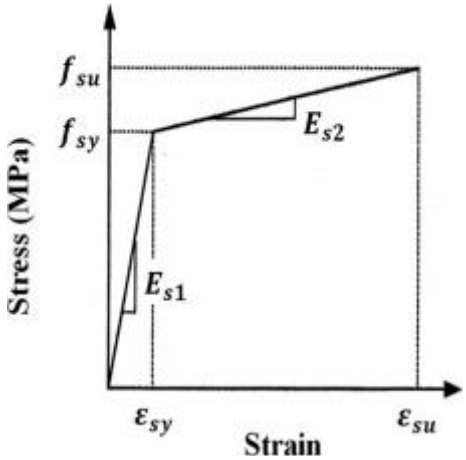

Fig. 3. Bi-linear stress-strain relationship.

exceeding DBE for a dominant failure mode, the support elements may be damaged, and the support system may behave in the elasto-plastic range. In this case, the natural frequency of the piping system is significantly reduced, and the response acceleration decreases while the response displacement increases. Accumulation of plastic deformation

Table 1
Parameters for parametric study.

Condition	Analytical case	Number of cases
Material model	SS400, SM570, low yield strength steel	3
Effective number of turns	3, 4, 5, 6, 7, 8, 9, 10	8
Wire diameter	20, 40, 60 mm	3
Coil index	3, 4, 5, 6, 7, 8, 9, 10	8
Pitch/Wire diameter	0.1–0.6	11
Total cases		6336

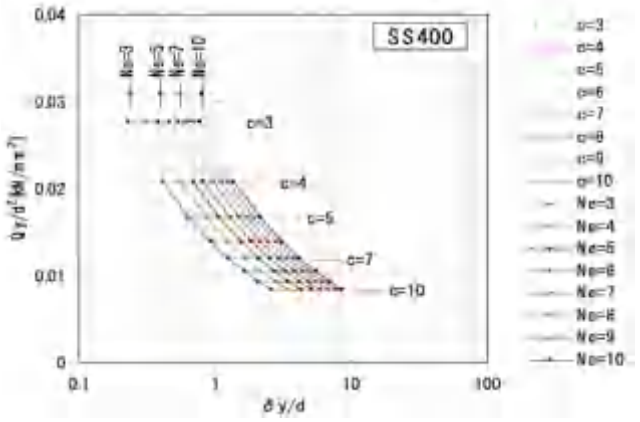

(a) Relation between load and deformation at yield point

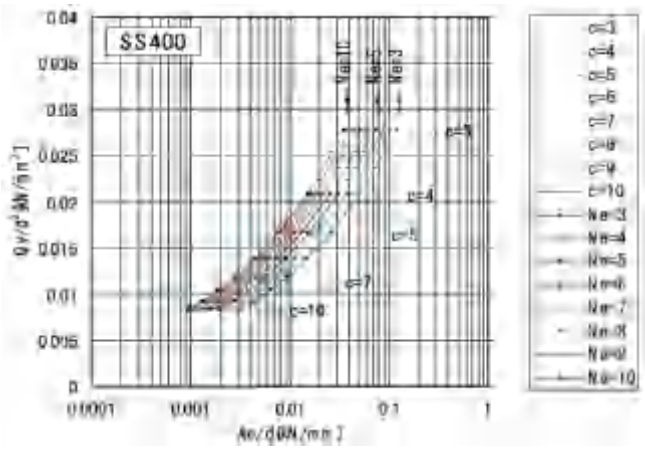

(b) Relation between load and spring constant at yield point

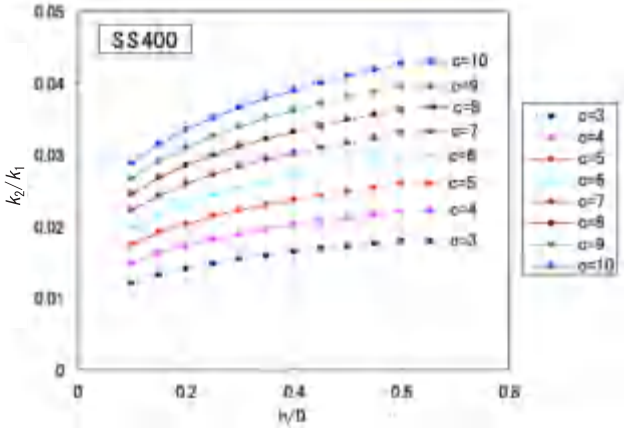

(c) Relation between stiffness ratio and h/D ratio of the coil

Fig. 4. Design diagrams for elasto-plastic SCD.

Table 2
Experimental specimens used for the loading test.

Element	(a)	(b)	(c)	(d)
Wire rod	SS400	SUP	SS400	SWRM
Wire diameter [mm]	16	8	6	6
Mean diameter of coil [mm]	76	50	43	43
Effective number of turns	3	8.5	5	5
Total number of coils	6	15.5	8	8
Free length [mm]	220	220	234	234
Primary rigidity [kN/m]	491	37.9	32.0	32.0
Secondary rigidity [kN/m]	19.6	–	1.28	1.28
Yield displacement [mm]	6	–	10	10
Yield load [kN]	2.94	–	0.320	0.320
Bilinear factor	1/25	–	1/25	1/25
Maximum displacement	100	80	60	60
Maximum load [kN]	4.79	3.03	0.384	0.384

due to repeated loading by long duration earthquake and multiple aftershocks can break pressure boundaries and cause radiation to leak. Therefore, in order to maintain the original function under the excitation by a large earthquake, it is more effective to reduce the response displacement by improving the damping performance rather than reducing the primary stress by improving the strength of the piping system. This design method is a new concept, but it is expected to be very effective in improving capacity and maintaining functionality.

The conventional seismic design method increases the apparent strength by rigidly connecting the building structure and piping to limit the deformation within the elastic range. However, in order to suppress the response of the piping to the elastic range, it is necessary to install a large number of rigid supporting parts and add expensive elements. This may bring problems such as reducing workspace for the plant operators and restraining thermal expansion of the piping. Therefore, the stiffened piping system is not effective as a measure for seismic retrofitting.

Some response control systems have been used to reduce the vibration of pipes, including snubbers, pipe hangers, support systems, isolators and so on. Park et al. (1997a,b) studied the energy absorbing capacity of the main steam and feedwater lines with conventional snubbers and energy absorbing supports. Parulekar et al. (2002) performed analytical and experimental research using elasto-plastic dampers to reduce the vibration of the piping and equipment of an NPP. An analytical study of a piping system with Stockbridge dampers was performed by Chang et al. (2016). Abe et al. (2003) developed a characteristic equation for a Lead Extrusion Damper. Three control devices for piping systems were proposed by Kunieda et al. (1987). A snubber and seismic stops were proposed by Olson and Tang (1988) for application to the NPP piping system.

In accordance with the increase of design earthquake level, it is thought to be reasonable to install a vibration control system to actively absorb seismic energy and obtain damping effects against the seismic motion of a beyond design earthquake. Currently, the Japan Society of Mechanical Engineers is moving toward revising the standard so that elasto-plastic behavior of piping itself is allowed, but it is not accepted that the piping system should behave in elasto-plastic range in the design stage. Therefore, it is necessary to analyse the dynamic behavior of the piping system during an earthquake using a vibration control device that can clearly grasp the elasto-plastic behavior from the design stage. However, few studies have been conducted on damping systems of piping (Takahashi et al., 2010). Fukasawa et al. (2008a,b) studied analytical models of coiled springs.

This study suggests an elasto-plastic SCD to control the response of the piping system under huge earthquake motion. The design method of SCD is introduced in this paper. The actual margin of the piping system with SCD under severe accident condition is evaluated through seismic analysis for multi input motion on the piping system in an NPP. Based on an examination on the piping system, including response control elements, this paper discusses the starting phase of research on seismic safety and function maintenance margin evaluation technique of a real piping system in a BDBE event.

2. Elasto-plastic steel coil damper

To review the function maintenance and seismic safety of the piping system under external event due to BDBE, it is necessary to consider the failure mode of the piping system. When designing piping systems, the primary stresses are first considered, and the fatigue resistance is investigated. Current critical piping systems in NPPs are secured for the required design strength by providing many support elements and support points. In order to review the failure mode of the piping system due to an external event, it is noted that the natural frequency of the piping system is lowered, and the response displacement of the pipes increases when a type of support considered to have low strength capacity is damaged. As a result, it is anticipated that the plastic ratio of the pipe and its supports will increase, and this will cause damage at the boundary. Therefore, it is important to reduce the seismic response of the piping against external events.

Under current design practice, during the normal operation of a plant, a snubber is installed on pipe supports in order to accommodate the thermal transformation of the pipes and confine the response displacement of the pipes during an earthquake. However, the supports held up by the snubber have low ductility and it is difficult to expect them to maintain functions necessary to respond to design external events or to secure seismic margin. Thus, in order to ensure the safety margin of the pipe system regarding design external events, it is essential to implement functions to accommodate thermal transformation under normal operation by adding a damping effect to the pipe system and reduce the maximum response displacement in the event of a huge earthquake beyond the scope of anticipated design.

To meet this requirement, this study developed a response control device that effectively utilizes the inherent elastic characteristics and the energy absorption capacity in plastic range. The device is a very simple structure that is formed by winding a metal wire into a coil. The thermal deformation of the coil spring during operation can be absorbed by the elastic deformation, and the energy absorption performance in the plastic range can be expected when an unanticipated large earthquake is input.

The elasto-plastic SCD has a very high damping capability because

(a) SCD A (b) SCD B (c) SCD C (d) SCD D

Fig. 5. SCD specimens of loading test.

Fig. 6. Experimental set-up of loading test.

the stress of the coil is uniformly distributed, without stress concentration, and the entire coil spring can be used as a damping element to utilize the hysteresis characteristics of the metal material. As a result, the fatigue strength of the damper is greatly improved, and the economic life cycle becomes longer.

Fig. 1 shows the general shape and dimensions of the coil spring to be developed for the design formulas of the SCD. When the spring is compressed by an external force, P, a torsional force, T is developed inside the spring, as shown in Fig. 2. The torsional force will generate torsional stress in the wire. The stress and strain relations of the bilinear spring are shown in Fig. 3.

The elastic spring constant of a coil spring, $\boldsymbol{k_{e1}}$ is represented by Eq. (1), and the elastic torsional stress, $\boldsymbol{\tau}$ is expressed in Eqs. (2).

$$k_e = \frac{Gd^4}{8N_eD^3} \tag{1}$$

where

d: wire diameter
N_e: effective number of turns,
D: mean diameter of coil (= 2R)
G: shear modulus of steel

$$\tau = \frac{8k_e\delta_y DW}{\pi d^3} \tag{2a}$$

where

δ_y: yield deformation
W: Wahl correction coefficient

$$W = \frac{4C-1}{4C-4} + \frac{0.615}{C} \tag{2b}$$

where

δ_y: yield deformation
W: Wahl correction coefficient
C: spring index(= D/d)

Wahl correction coefficient W is one of the possible correction factors to consider the transverse force shear stress and stress concentration due to curvature. Thus, the W can be replaced by $\left(1+\frac{d}{2D}\right)$. From Eqs. (1) and (2), the yield displacement is obtained as Eq. (3).

$$\delta_{y1} = 2.63\frac{\tau}{E_{s1}}\pi DN_e\left(\frac{D}{d}\right) \tag{3}$$

where

E_{s1}: elastic modulus of steel before yielding (Fig. 1)

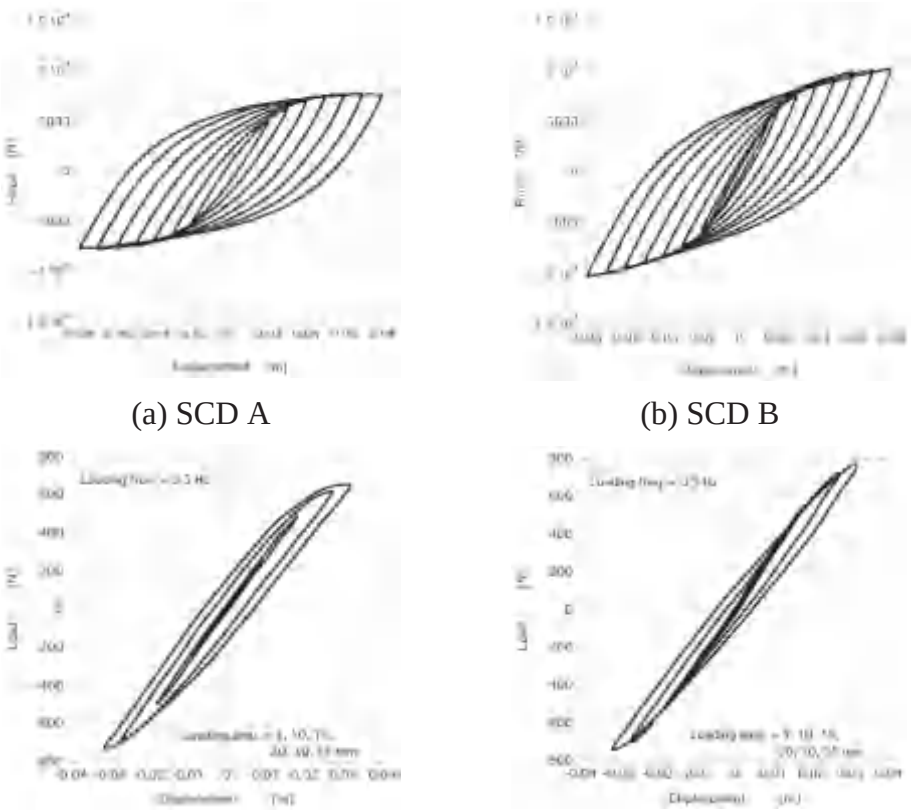

(a) SCD A (b) SCD B

(c) SCD C (d) SCD D

Fig. 7. Comparison of hysteresis characteristics using different types of specimen.

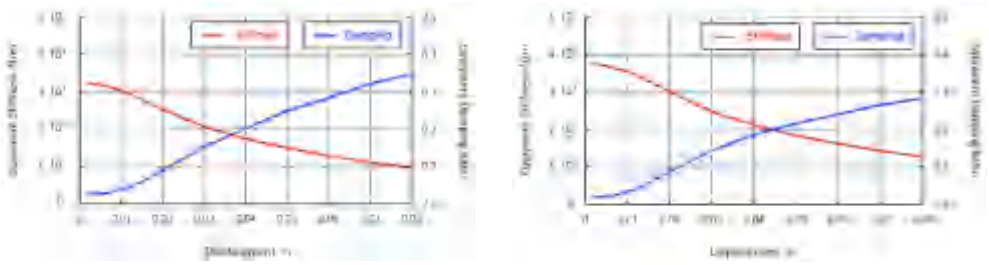

(a) SCD A (b) SCD B

Fig. 8. Comparison of mechanical characteristics in displacement dependency.

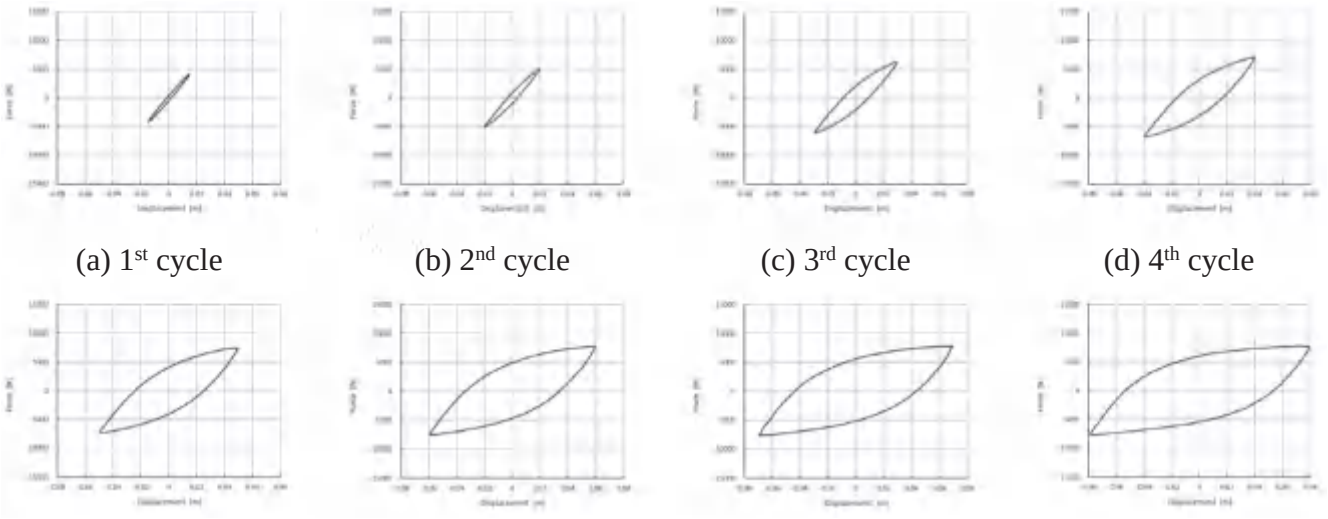

(a) 1st cycle (b) 2nd cycle (c) 3rd cycle (d) 4th cycle

(e) 5th cycle (f) 6th cycle (g) 7th cycle (h) 8th cycle

Fig. 9. Hysteresis loops obtained from loading test of specimen A.

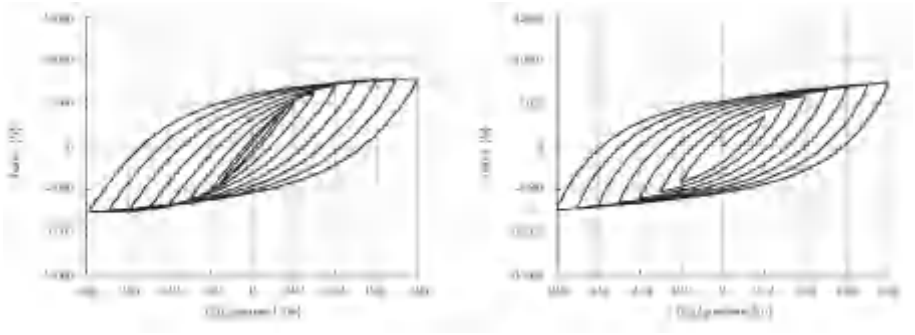

(a) Experiment (b) Analysis

Fig. 10. Hysteresis loops obtained from analysis and experiment.

N_e: effective number of turns

In a different way, the yield deformation is derived from the relation between the yield strain and the material strength.

$$\delta_{y2} = \varepsilon_{sy}\pi DN_e = \frac{f_{sy}}{E_{s1}}\pi DN_e \tag{4}$$

where

ε_{sy}: yield strain
f_{sy}: yield stress

The yield strength of a wire under axial deformation is expressed by the following equation.

$$F_{sy} = f_{sy}\frac{\pi d^2}{4} \tag{5}$$

where

F_{sy}: yield strength

Therefore, the elastic stiffness is obtained as Eq. (6).

$$k_{e2} = \frac{F_{sy}}{\delta_{y2}} = E_{s2}\frac{\pi d^2}{4}\frac{1}{\pi DN_e} \tag{6}$$

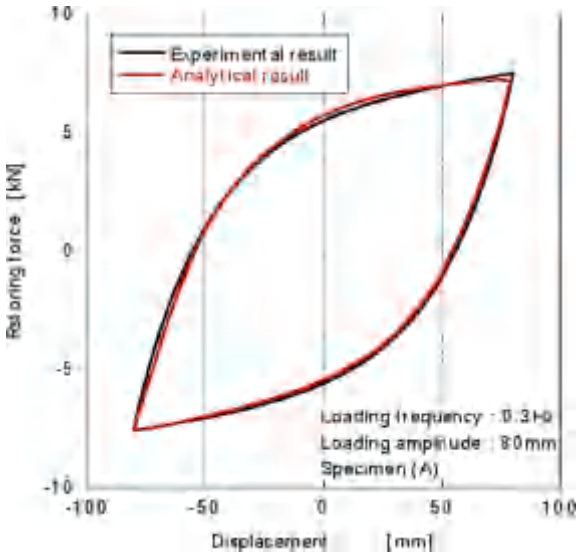

Fig. 11. Comparison of analytical and experiment hysteresis loops.

where

E_{s2}: elastic modulus of steel after yielding (Fig. 1)

In order to develop the design equation of an elasto-plastic SCD, this study expanded the theoretical equation used in the elastic range into the elasto-plastic range. Accordingly, parameters p_1, p_2, and p_3 for elasto-plastic design are added in Eqs. (3) and (6) as follows.

$$\delta_{y1} = p_1\left[\frac{f_{sy}}{E_{s1}}\pi DN_e\left(\frac{D}{d}\right)^{P_2}\left(\frac{h}{d}\right)^{P_3}\right] \tag{7}$$

$$\delta_{y2} = p_1\left[\frac{f_{sy}}{E_{s2}}\frac{\pi d^2}{4}\frac{1}{\pi DN_e}\left(\frac{D}{d}\right)^{P_2}\left(\frac{h}{d}\right)^{P_3}\right] \tag{8}$$

where

h: pitch ($=T_e/N_e$) (Fig. 1)
T_e: effective deformation part ($=hN_e$) (Fig. 1)

After determining the parameters, the SCD can be designed using Eqs. (7) or (8). However, the constant parameters p_1, p_2, and p_3 cannot be easily obtained by theoretical equations. In order to determine the parameters, this study performed 6336 experiments considering the variables of effective number of turns, wire diameter, and spring index as shown in Table 1. The parameters were determined by optimization method using the least-square approach, as shown in Eq. (9).

$$\min_p \frac{1}{2}\left\|\delta_y(p_1, p_2, p_3; f_{sy}, E_{s1}, E_{s2}, t, d, D, h) - \delta_{y,analysis}\right\|_2^2$$
$$= \min_p \frac{1}{2}\sum_i \delta_y\{(p_1,\ p_2,\ p_3;\ f_{sy}^i,\ E_{s1}^i, E_{s2}^i, t^i, d^i, D^i, h^i) - \delta_{y,analysis}^i\}^2 \tag{9}$$

The residual error is the difference between the finite element analysis results and the experimental results. In Eq. (9), $\delta_{y,analysis}$ is the true deformation obtained from the finite element analysis of the coil spring. The prediction formula for the fundamental mechanical design characteristics of an elasto-plastic SCD was set up from the parametric study.

$$\delta_y = 1.91\frac{f_{sy}}{E_{s1}}\pi DN_e\left(\frac{D}{d}\right) \tag{10}$$

The yield deformation in Eq. (10) is a very important design parameter in this research. This yield deformation determines the allowable thermal expansion range and the expected elasto-plastic range to absorb the energy of the design external event.

$$F_y = 0.36f_{sy}\frac{\pi d^2}{4}\left(\frac{D}{d}\right)^{-1} \tag{11}$$

The yield strength represents the load resistance of the piping system. The 1st stiffness of the system within the allowed thermal expansion range in operation is represented by:

$$k_e = 0.19\frac{\pi d^2}{4}\frac{1}{\pi DN_e}\left(\frac{D}{d}\right)^{-2} \tag{12}$$

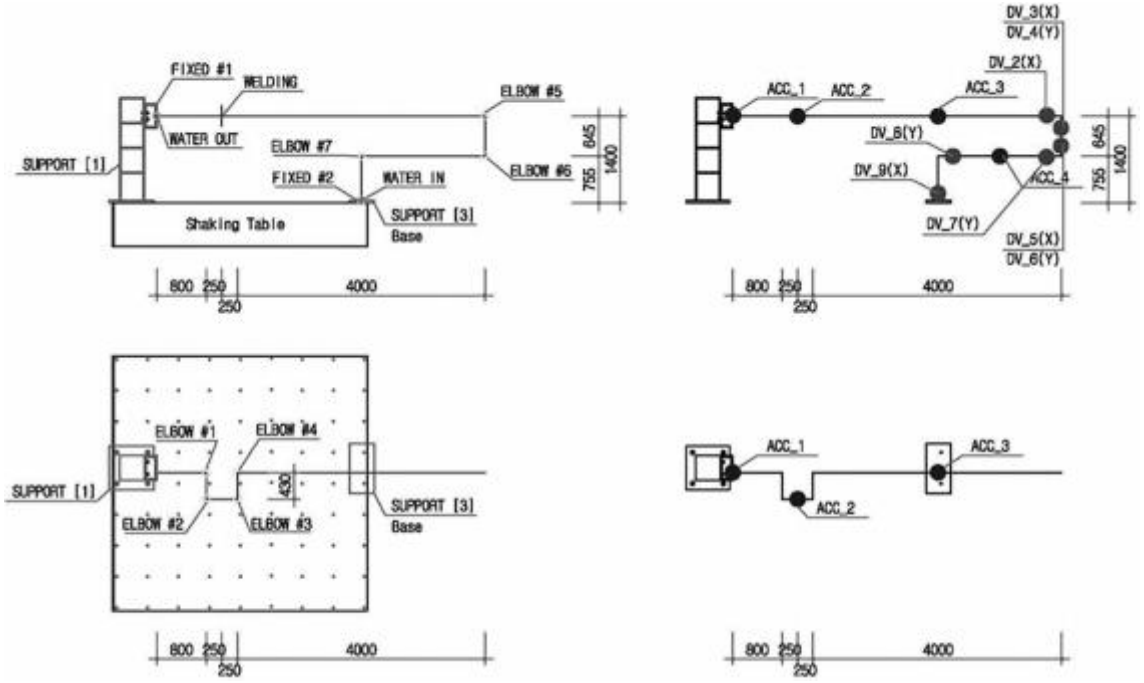

Fig. 12. Experimental apparatus for analytical model of piping system.

Fig. 13. Experimental set-up for piping system on the shaking table.

Fig. 14. FE Model of the piping system using ABAQUS.

Table 3
ABAQUS Modeling (PIPE31 Element, Internal Pressure 20 MPa (20.5 ℃), Section Properties).

Pipe size (in.)	External diameter (mm)	Internal diameter (mm)	Nominal thickness
2	60.3	42.8	8.74
3	88.9	66.6	11.13

Table 4
Material properties.

Mass density (N/mm^3)			Young's Modulus	Poisson's ratio	Material Damping (%)
Stainless steel	steel	Water			
8.0E − 9	7.8E − 9	1.0E − 9	199,000	0.3	4

Eq. (13) represents the second stiffness.

$$k_p = 0.024\left[E_{s1}\frac{\pi d^2}{4}\frac{1}{\pi D N_e}\right]\left(\frac{D}{d}\right)^{-1.28}\left(\frac{h}{D}\right)^{0.22}\left(\frac{E_{s1}}{E_{s2}}\right)^{-0.75} \quad (13)$$

where

F_y: yield load
k_p: plastic spring constant

Fig. 4 shows the design parameter characteristics of the elasto-plastic SCD when using SS400 material.

3. Loading test of elaso-plastic coil damper

3.1. Experimental specimen

Loading test was performed to evaluate the fundamental mechanical characteristics of the SCD. Four different elements were prepared to manufacture the specimen. Table 2 shows the specifications of the elements. As can be seen in Fig. 5, four different specimens were manufactured for the loading test using the elements in Table 2. Specimen A shows the basic type of SCD using SS400 as a wire rod. As a combination of elements (a) and (b), specimen B was manufactured to investigate the restoring performance against the residual displacement by installing a coil spring into the SCD. Specimens C and D are test specimens used to compare the hysteresis characteristic of SS400 and SWRM which are commonly used for the elasto-plastic damping materials.

3.2. Experimental method

Hysteresis characteristics of the test specimen were first obtained through the loading test. Next, the dependencies of displacement and frequency on the mechanical characteristics were investigated using the test results. Fig. 6 shows the loading test conditions set for the hydraulic servo actuator. The displacement transducer and load cell installed in the hydraulic servo actuator system were used to measure the displacement and the force.

To record the hysteresis characteristics data, the specimens were compressed and tensioned by repeated cycling loading with different loading frequencies and amplitudes. The displacement amplitude of loading ranged from 2 mm to 80 mm. The main loading frequency was 0.3 Hz. The loading frequency ranged from 0.05 Hz to 0.5 Hz according to the maximum velocity performance of loading apparatus. The sampling frequency (Randal, 1987) of the signal recorded by the data logger was set at 50 Hz in lower loading frequency and 100 Hz in the higher loading frequency. In addition, the temperature on the surface of the damper specimens was measured before and after the loading test using a contact-type thermometer.

3.3. Experimental results

Fig. 7 shows one set of experimental results from the loading tests. Fig. 7(a) and (b) show the comparison of damping performance for a large deformation area for specimens A and B. Specimen B increases the spring constant by adding an elastic coil spring to specimen A. However, it was confirmed that both damping performances have stable elasto-plastic damping characteristics, even in a large deformation region.

Fig. 7(c) and (d) provide a comparison of the hysteresis characteristics using different types of wire rods for specimens C and D. It was confirmed that specimen C using the SS400 wire rod has restoring force characteristics very similar to those of specimen D, which uses a low yield strength steel that is widely used for elasto-plastic damper. It should be noted that SWRM is much more expensive than SS400. Therefore, the damper using SS400 as the elasto-plastic material can deliver good quality for effective damping performance and cost reduction.

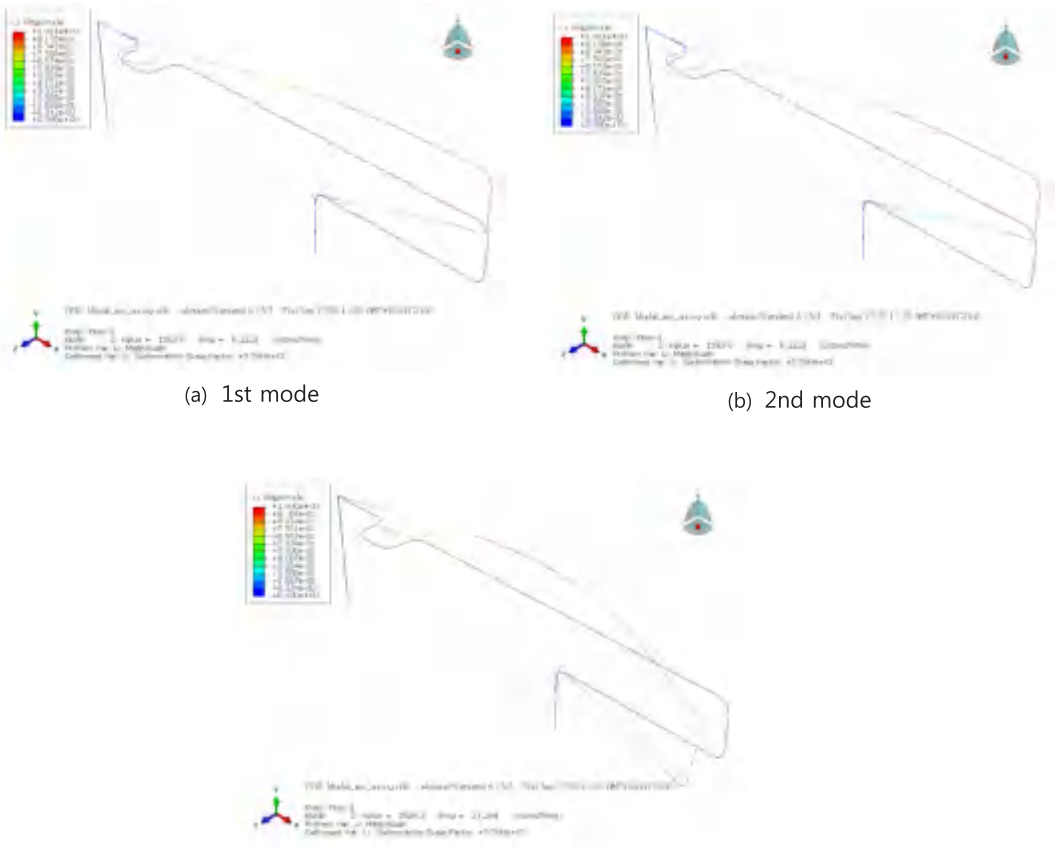

(a) 1st mode (b) 2nd mode

(c) 3rd mode

Fig. 15. Mode shapes of the piping system.

Table 5
Mode analysis result.

Component	Mode (N)/Resonant Frequency (Hz)				
	1	2	3	4	5
Experiment	3.35	5.59	10.34	14.74	20.64
Analysis	3.41	6.33	11.28	16.41	23.36
Exp./Anal.	0.98	0.88	0.92	0.90	0.88

Fig. 8 compares the mechanical characteristics of displacement dependency using specimens A and B. It was confirmed that each damper has specific mechanical characteristics suitable for the damper design. The figure shows that the stiffness (red line) degrades but the damping performance (blue line) increases after the yield displacement is exceeded. It was confirmed that the damper manufactured in this study can control the allowable range of elastic thermal expansion and the elasto-plastic deformation range to ensure the function and the seismic safety of the piping system. Fig. 9 shows the hysteresis loops in the case of specimen A. As the amplitude of the loading displacement increases the hysteresis loop area increases.

4. Examination of analytical model

This study proposes Formulas (10)–(13) for the design of SCD and verifies the validity of these formulas through experiments. However, in order to conduct detailed assessment of the performance of the pipe system and seismic margin against design external events, it is necessary to conduct time history analysis using an input earthquake motion or floor response motion. In general, time history response analysis often applies the load-displacement properties of the bilinear model using design Formulas (10)–(13). However, the load-displacement properties of the bilinear model pose problems in obtaining the maximum response acceleration or maximum response displacement because the turning point of the first and second stiffness becomes discontinuous.

Thus, to fully express the load-displacement properties of the SCD, a more reasonable analytical damping model is required. This study selected the Rate Model (Bhatti and Pister, 1981) to express the damping force. Eqs. (14) through (17) are the formulas of the Rate Model.

$$\dot{F}(t) = k_1\dot{x}(t)\{1 - \mathrm{sgn}(\dot{x}(t))(F(t)/F_y - S(t))^n\} \tag{14}$$

$$S(t) = \frac{k_2}{F_y/X_y - k_2}\left(\frac{x(t)}{X_y} - \frac{F(t)}{F_y}\right) \tag{15}$$

$$F_y = k_1 X_y \tag{16}$$

$$k_2 = \gamma k_1 \tag{17}$$

where

$F(t)$: force in SCD
k_1: first stiffness of SCD
k_2: second stiffness of SCD
$x(t)$: displacement of SCD
$\dot{x}(t)$: velocity of SCD
F_y: yield force
X_y: yield displacement
n: material parameter

As a differential equation, compared to using a bilinear typed model, the Rate model produces higher precision of estimates in terms of maximum response acceleration and maximum response

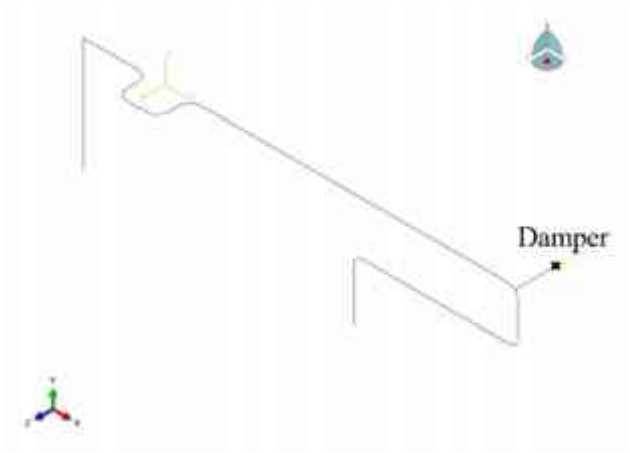

(a)EW direction

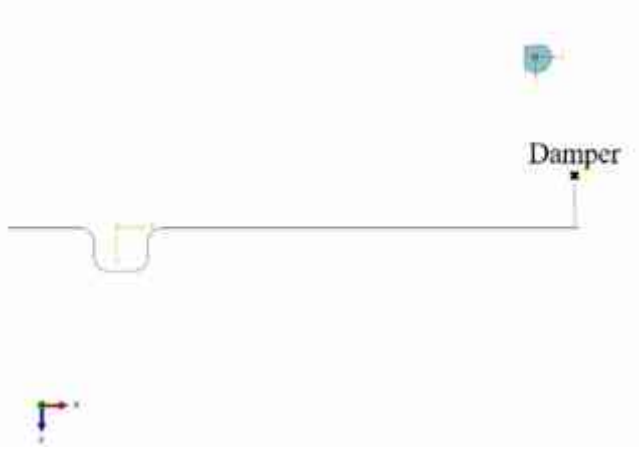

(b) NS direction

Fig. 16. Location of damper.

Table 6
Damper properties in the analytical model.

1st stiffness (k_1)	2nd Stiffness (k_2)	Yield Strength (f_y)	Yield Displacement (u_y)
73.5 N/mm	2.45 N/mm	1190 N	16.2 mm

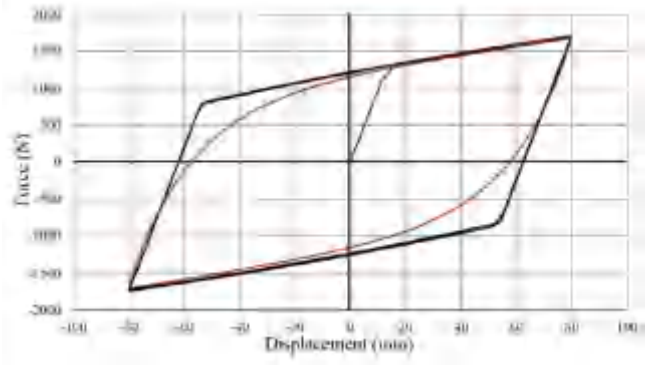

Fig. 17. Hysteresis roof of the damper in the analytical model.

displacement in expressing the load-displacement properties. In this regard, the Rate model is a more efficient model when considering maximum response to design external events as examined in this study.

The sharpness of the transition from the elastic to the inelastic region of the Rate model is controlled by the material parameter, n. If n approaches infinity, this model will be a bilinear model. Fig. 10 shows hysteresis loops obtained from loading tests and analysis using the Rate model. Fig. 11 compares analytical and experimental hysteresis loops in the case of specimen A. 0.3 Hz of loading frequency and 80 mm of loading displacement were applied as experimental condition. As can be seen in the figure, the analytical results match well with the experimental results.

5. Dynamic response analysis

The thermal expansion is critical to piping support design and seismic response. Considering that the linear thermal expansion coefficient is 16.0e − 6/℃, and pipe length is 10 m, when the temperature rises from 20 ℃ to 200 ℃, a deformation of 28.8 mm occurs. As the elasto-plastic damper suggested herein is of coil type, the thermal deformation of the pipe can respond with constant stress over the whole coil length. In addition, as the thermal expansion can be estimated at the design stage, the engineer can set the yield displacement and design the shape of the coil accordingly. Thus, during severe accident, deformation due to thermal expansion can be accommodated with elastic deformation of the coil. By doing so, system can simultaneously respond to both thermal expansion and earthquake motion.

This study analysed the effects of the coil damper on the dynamic response of the piping system. For the study, a simple piping system was designed and tested on the shaking table to identify the modal frequencies. The piping system was pressurized with water at room temperature. This piping system consists of 2-inch diameter and 3-inch diameter pipes, elbows, and reducers. Fig. 12 shows the layout of the model and the locations of the sensors used to measure the displacement and acceleration. Fig. 13 shows the experimental set-up on the shaking table. Broad band random motions with frequency range of 0.5–50 Hz and RMS (root mean square) magnitude of 0.1 g were applied as table motions along 3 axes.

The analytical model was also constructed as shown in Fig. 14. ABAQUS PIPE31 elements were used to express the model. The element sizes and material properties are shown in Tables 3 and 4. The analytical model was validated by comparing the modal frequencies obtained from the analysis and the test. Fig. 15 shows the fundamental mode shapes obtained from eigen analysis. Table 5 compares the modal properties obtained from the analysis and experiment. The modal analysis results agree well with the experimental results.

Dynamic analyses were performed before and after adding the coil spring damper to the analytical model at the location shown in Fig. 16. The damper was attached next to the reducer. The damper properties are shown in Table 6 and Fig. 17. A harmonic motion was input at the base. The time history acceleration and response spectrum are shown in Fig. 18. Table 7 and Figs. 19 and 20 compare the analyses results for the models with and without damper. In the table and figures, the fixed case means the rigid support condition at the damper position. The analysis results show good control performance of the damper for dynamic motion

6. Conclusion

This study investigates a response control system using an elasto-plastic damper as a preventive technology against severe accidents of the piping system in NPPs. SCD is recommended to control the dynamic response of the NPP piping system for a huge earthquake exceeding DBE. This paper introduced a design method of an elasto-plastic damper and determined its mechanical characteristics through loading test and analytical study. Then, this study suggested an analytical model to represent the vibration characteristics of the elasto-plastic SCD.

Actual piping systems with and without SCD were modeled using finite element method. Experimental modal identification was also performed to validate the analytical model. The performance of the SCD

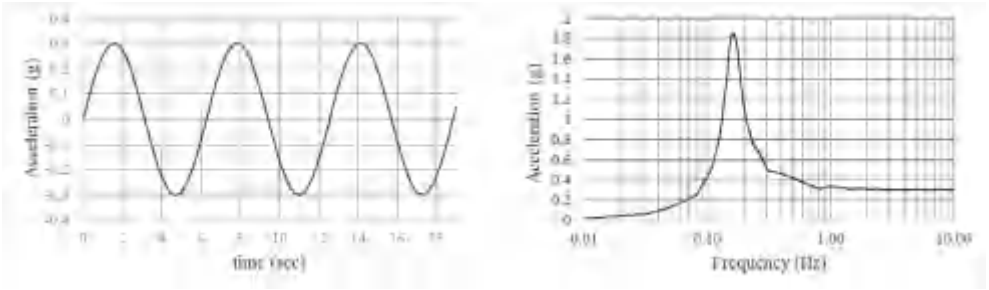

(a) Time History (b) Response Spectrum

Fig. 18. Dynamic Input Motion for the analytical model.

Table 7
Comparison of dynamic analysis results.

	without damper		with damper (SCD)
	free	fixed	
Relative Displacement (mm)	9.59	7.36	0.57
Stress (MPa)	30.30	28.14	24.41
Acceleration (g)	0.337	0.297	0.793

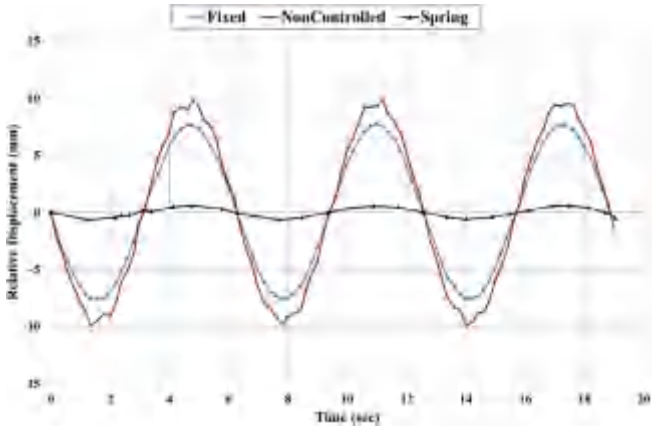

Fig. 19. Relative displacement of the pipe system with and without of damper.

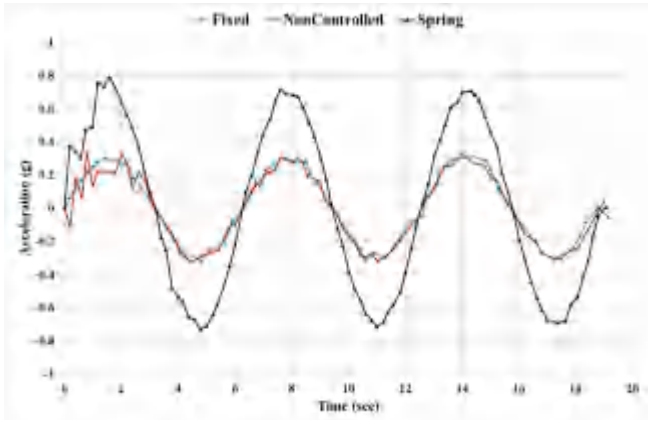

Fig. 20. Acceleration of the pipe with and without of the damper.

was proven by the analyses. Controlled responses of the piping system model were compared with uncontrolled responses. From the dynamic analysis results, it was confirmed that the SCD can effectively reduce the vibration of the piping system under dynamic motion. When elasto-plastic supports are adopted for pipe systems, it becomes possible to control the elastic response of the pipes, establish countermeasures against thermal expansion under normal operation, and maintain functions and secure safety when the pipes of nuclear facilities are affected by any vibratory ground motion exceeding the design criteria.

Acknowledgements

This work was supported by the energy technology development program of Korea Institute of Energy Technology Evaluation and Planning (KETEP) Grant funded by the Korea Government (MOTIE) (No. 20181520102780). The authors would like to express their appreciation for the financial support.

References

Abe, H., Ichihashi, I., Kuroda, K., Iwatsubo, T., Tai, K., 2003. “Seismic proving test of heavy component with energy absorbing support”. In: Proceedings of the International Conference on Global Environment and Advanced Nuclear Power Plants, Kyoto, Japan, September 2003.

Bhatti, M.A., Pister, K.S., 1981. A dual criteria approach for optimal design of earthquake-resistant structural systems. J. Earthquake Eng. Struct. Dyn. 9, 557–572 John Wiley & Sons.

Chang, S., Sun, W., Cho, S.G., Kim, D., 2016. Vibration control of nuclear power plant piping system using stockbridge damper under earthquakes. Sci. Technol. Nucl. Install. 201 Article ID 5014093.

Fukasawa, T., Fujita, S., Kurabayashi, H., Kinoshita, A., 2008a. Study of earthquake isolation system using vertically utilized coiled springs – 1st report, static tests for elastic coiled spring(mechanical systems). J. Jpn. Soc. Mech. Eng., Vol. C 74 (739), 506–512 (in Japanese).

Fukasawa, T., Fujita, S., Kurabayashi, H., Kinoshita, A., 2008b. Study of earthquake isolation system using vertically utilized coiled springs: 2nd report, quashi-static tests for elasto-plastic coiled springs. J. Jpn. Soc. Mech. Eng., Vol. C 74 (739), 513–520 (in Japanese).

Kojima, N., Tsutumi, Y., Yonekura, K., Nishino, K., Watanabe, Y., Kumagai, S., Kamino, H., 2017. “Seismic Test Result Of Motor- Operated Valve Actuators For Nuclear Power Plant”. In: Proceedings of ASME PVP Conference, Volume 8: Seismic Engineering, Paper No. PVP2017-65600.

Kojima, N., Tsutumi, Y., Yonekura, K., Nishino, K., Watanabe, Y., Kumagai, S., Kamino, H., 2018. “Seismic Test Result of Motor-Operated Butterfly Valve Actuators for Nuclear Power Plant.” In: Proceedings of ASME PVP Conference, Volume 8: Seismic Engineering, Paper No. PVP2018-84219.

Kunieda, M., Chiba, T., Kobayashi, H., 1987. Positive use of damping devices for piping systems-some experiences and new proposals. Nucl. Eng. Des. 104 (2), 107–120.

Miyano, H., Takagi, T., Sakai, S., 2009. The research committee of Chuetsu-Oki earthquake influences to Kashiwazaki − Kariwa nuclear power station (seismic margin on nuclear power station design). Trans. Jpn. Soc. Mech. Eng. Ser., B 75 (751), 450–452.

Nakamura, I., 2013. “Seismic Seismic Safety Capacity of a Piping System with Pipe Supports Based on the Shake Table Test”. In: Proceeding of ASME Pressure Vessels and Piping Division Conference, PVP2013-97852.

Olson, D.E., Tang, Y.K., 1988. Decreasing snubber in-service inspection costs through snubber reduction and improved test limits. Nucl. Eng. Des. 107 (1-2), 183–199.

Park, Y.J., DeGrassi, G., Hofmayer, C.H., Bezler, P., Chokshi, N.C., 1997a. Analysis of nuclear piping system seismic tests with conventional and energy absorbing supports. K15-3, Trans. SMiRT 14.

Park, Y.J., Hofmayer, C.H., Chokshi, N.C., 1997b. Application of Equivalent Linearization Approaches to Nonlinear Piping Systems. K17-4, Trans. SMiRT 14.

Parulekar, Y.M., Reddy, G.R., Vaze, K.K., Kushwaha, H.S., 2002. Elasto-plastic Damper for Passive Control of Seismic Response of Piping Systems. BARC Internal Report, Reactor Safety Division.

Randal, R.B., 1987. Frequency Analysis. Brüel & Kjaer.

Sakai, M., Kanazawa, K., Ohtori, Y., 2016. “Development of High Acceleration Shaking Table System Using Resonance Vibration.” In: Proceedings of ASME PVP Conference,

Volume 8: Seismic Engineering, Paper No. PVP2016-63752.
Takahashi, T., Maekawa, A., Suzuki, M., 2010. Effect of elastic-plastic support on seismic response of piping system. In: The Proceedings of the Dynamics & Design Conference Volume 2010. JSME, pp. 421.
Takahashi, T., Maekawa, A., 2012. Seismic response of piping systems utilizing plastically deformable pipe support structures. INSS J. 19 (2012 NT-4), 75–83 (In Japanese).
Takahashi, T., Maekawa, A., 2014. Seismic response evaluation for piping systems with support structures (Effect of Input Acceleration Amplitude on Resonance Frequency and Response Reduction in the Elastic Vibration Test). INSS J. 21 (2014 NT-2), 75–85 (In Japanese).